MPE Report Vol. 288, 159

Comparison of EPIC-pn ground-based and in-orbit calibration measurements

M. J. Freyberg[1], W. Burkert[1], G. Hartner[1], M. G. F. Kirsch[2], and E. Kendziorra[3]

[1] Max-Planck-Institut für extraterrestrische Physik, Garching, Germany

[2] ESAC, ESA, Villafranca, Spain

[3] Institut für Astronomie und Astrophysik, Universität Tübingen, Tübingen, Germany

1. Introduction

The EPIC-pn CCD camera aboard XMM-*Newton* has been extensively calibrated on ground as well as in orbit. While the formal *flight spare model* (FS) is in operation on XMM-*Newton*, the *flight model* (FM1) is situated at the *Panter* X-ray Test Facility. This allows additional tests of the detector performance and comparison of ground calibrations prior to launch with present measurements. Additionally, tests can be performed without loss of scientific XMM-*Newton* observing time.

Here we present recent results on a comparison of the internal camera background at low energies in various instrument read-out modes, on the precise determination of frame times and EPIC-pn oscillator frequency, and on the determination of charge losses during fast shifts (read-out of EPIC-pn window modes).

2. EPIC-pn low-energy background

For various instrument modes the low-energy background spectra and intensity levels have been determined for EPIC-pn FM1 (PANTER) and FS cameras (XMM-*Newton*, closed filter observations). Figure 1 summarizes these results for FM1 (left) and FS (right), with spectra (top) and intensities (bottom) for each read-out mode.

Spectra for each camera are comparable in shape. The in-orbit spectra (FS, after MIP rejection) are steeper than for FM1 below 30 adu (1 adu $\sim$ 5 eV). Low-energy background intensities are closely related to the number of read-outs per second and thus the background is dominated by electronic read-out noise. A simple 2-parameter model has been fit to the standard imaging modes (labelled in blue). On ground longer integration times (extended full-frame mode with longer wait time between quadrant read-outs) are available than in orbit, the lower threshold can also be set to lower values (16 rather than 20 adu). For soft and faint diffuse sources the extended full-frame modes are therefore best-suited. For sources that have their emission maximum below the lower event threshold pile-up of X-rays with background could lead to event amplitudes above the lower threshold and thus mimic a low-energy excess. To investigate this further, a special short calibration measurement has recently been performed with a lower threshold of 16 adu (NRCO-49, `0979_9097900002_PNU002`) to determine the low-energy background below the default event threshold of 20 adu. A comparison (see upper right panel in Fig. 1) of FS (filled red hexagons) and FM1 cameras (empty black hexagons) shows differences in the detailed spectral shape, however, at 16 adu the intensity levels agree.

3. EPIC-pn frame times and oscillator

EPIC-pn frame times for each instrument submode can be precisely determined independent of any oscillator properties using the integer-valued time stamps provided in the `PNAUX1` FITS extension, `FTCOARSE` (full seconds) and `FTFINE` (sub-seconds). The internal EPIC-pn oscillator has a nominal frequency

Send offprint requests to: M. J. Freyberg, e-mail: `mjf@mpe.mpg.de`

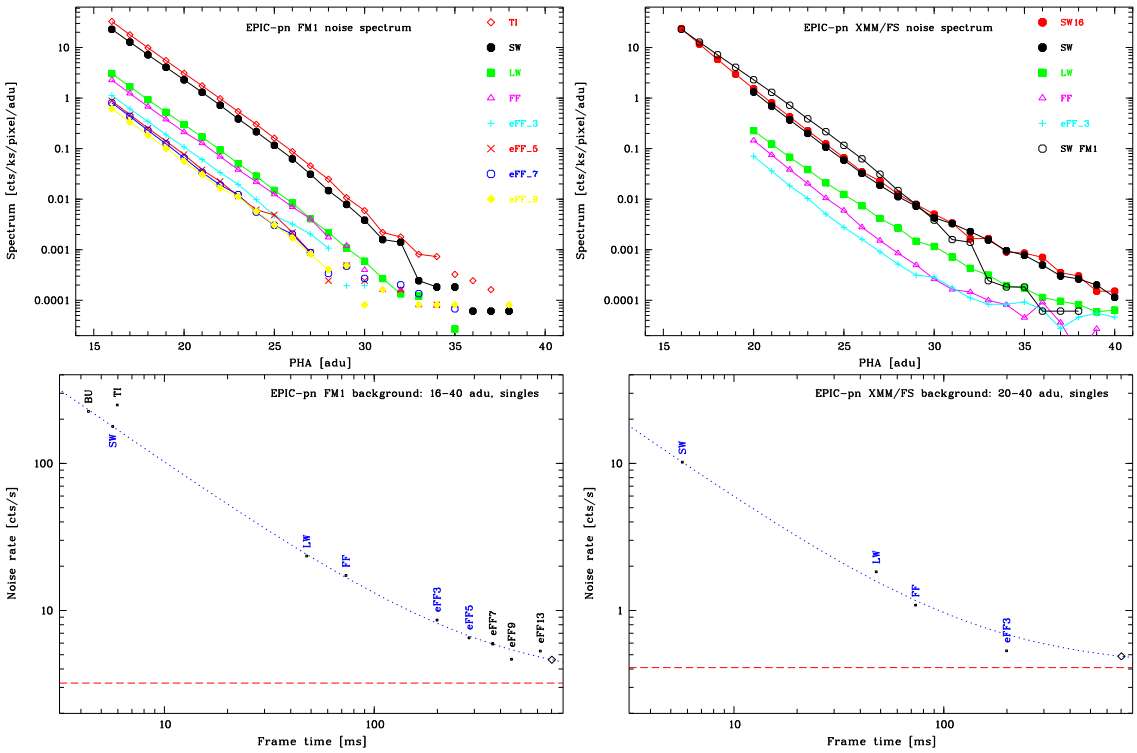

Fig. 1. *Top left:* internal background spectra of various instrument modes at the focal position for the FM1 camera at the Panter X-ray test facility. *Bottom left:* background intensity in the $16-40$ adu energy range for FM1 for various instrument modes. The blue dotted line is a two-parameter fit using the standard imaging modes only (SW, LW, FF, eFF_3, eFF_5; blue labels). *Right:* similarly for FS camera aboard XMM-*Newton* for the $20-40$ adu energy range. In the upper right panel a SW mode observation with the FS camera with lower threshold 16 adu is shown (filled red hexagons, NRCO-49) along with the corresponding spectrum for the FM1 camera (empty black hexagons). For details see text.

Table 1. EPIC-pn frame time analysis using the `PNAUX1` file for all read-out modes: the given nominal clock numbers (column 2) have been obtained from the nominal frame times (CCF values) multiplied by $f_{\mathrm{pn}} = 25\,\mathrm{MHz}$; the quantity M_1 is the average measured distance between two events in two consecutive frames within the same second in `FTFINE` units; multiplied by 512 it gives the number of clocks of the internal pn-oscillator for each read-out mode. The derived values differ from the values in the `EPN_TIMECORR` CCFs. In the columns at the right-hand-side we give recommended values for the length of each read-out cycle as well as for the frame time *assuming* a $f_{\mathrm{pn}} = 25\,\mathrm{MHz}$ internal pn-oscillator frequency.

Mode	clocks	Observation	$512 * M_1$	Δ	recommendation	
FF	1834108	0078_0124100101_PNS003	1834123.988	+16	1834124 clocks	73.36496 ms
eFF_5	7076988	0044_0119710201_PNS008	7077004.295	+16	7077004 clocks	283.08016 ms
eFF_3	4979836	0469_0108260201_PNS003	4979852.043	+16	4979852 clocks	199.19408 ms
LW	1191616	0537_0136540701_PNS008	1191595.994	−20	1191596 clocks	47.66384 ms
SW	141794	0908_0158961001_PNS013	141795.019	+1	141795 clocks	5.67180 ms
TI	149116	0807_0158971201_PNS003	149115.990	0	149116 clocks	5.96464 ms
BU	108614	0411_0153750501_PNS001	108612.031	−2	108612 clocks	4.34448 ms

of $f_{\mathrm{pn}} = 25\,\mathrm{MHz}$, but the exact value is unknown and subject of this analysis. The CCD sequencer and the `FTFINE` counter are both clocked by this oscillator. An external oscillator triggers the increment of `FTCOARSE` and the reset of `FTFINE`. $\delta_{\mathrm{aux}} \equiv 512/f_{\mathrm{pn}}$ is the length of a `FTFINE` unit, nominally $\delta_{\mathrm{aux}} = 20.48\,\mu\mathrm{s}$. As the mode sequences are not an integer multiple of 512 clocks the time stamps in the `PNAUX1` file show a jitter of 1 `FTFINE` unit.

For times of two events we have:
$T(n) = T_{\mathrm{coarse}}(n) * 1\mathrm{s} + T_{\mathrm{fine}}(n) * \delta_{\mathrm{aux}}$

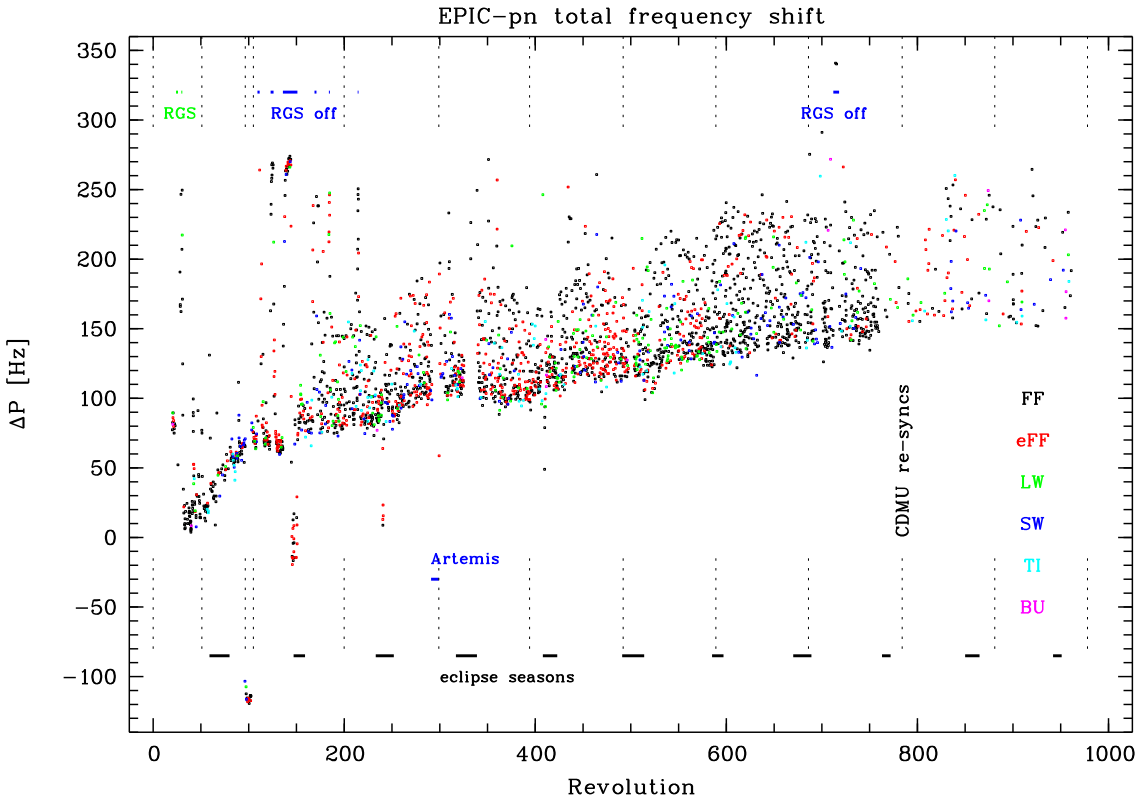

Fig. 2. Total difference of the effective frequency of internal EPIC-pn oscillator (combined with external OBT oscillator effects) from the nominal value of $f_{\rm pn} = 25\,{\rm MHz}$ as function of time and instrument mode. External events like eclipse seasons or RGS switch offs are indicated; dotted vertical lines show CDMU re-syncs. The long-term increase of the frequency is probably due to external temperature effects or to ageing the EPIC-pn oscillator. There is no apparent mode dependency.

$T(n+1) = T_{\rm coarse}(n+1) * 1{\rm s} + T_{\rm fine}(n+1) * \delta_{\rm aux}$.

The time difference is then

$T(n+1) - T(n) = [T_{\rm coarse}(n+1) - T_{\rm coarse}(n)] * 1{\rm s} + [T_{\rm fine}(n+1) - T_{\rm fine}(n)] * \delta_{\rm aux}$.

If these two events are within the same second and in two consecutive read-out cycles this reduces to:

$T_{\rm frame} = 0{\rm s} + [T_{\rm fine}(n+1) - T_{\rm fine}(n)] * \delta_{\rm aux}$

$T_{\rm fine}(n+1) - T_{\rm fine}(n) = T_{\rm frame}/\delta_{\rm aux}$.

When we average this (integer) quantity over the total exposure we can discard the jitter effect and the real value M_1 is

$M_1 := \langle T_{\rm fine}(n+1) - T_{\rm fine}(n) \rangle = T_{\rm frame}/\delta_{\rm aux}$.

If we now consider the similar case of 2 events separated by 1 frame time but for events with full-second increment in between, we get:

$T_{\rm frame} = 1{\rm s} + [T_{\rm fine}(n+1) - T_{\rm fine}(n)] * \delta_{\rm aux}$

$T_{\rm fine}(n) - T_{\rm fine}(n+1) = (1{\rm s} - T_{\rm frame})/\delta_{\rm aux}$

and to discard the jitter effect by averaging over all such occurrences within an exposure $M_2 := \langle T_{\rm fine}(n) - T_{\rm fine}(n+1) \rangle = (1{\rm s} - T_{\rm frame})/\delta_{\rm aux}$.

From these quantities M_1 and M_2 (in `FTFINE` units or 512 oscillator units) one can derive the effective oscillator periods and frame times via $\delta_{\rm aux} = 1{\rm s}/(M_1 + M_2)$ and $T_{\rm frame} = 1{\rm s} * M_1/(M_1 + M_2)$.

Table 1 illustrates the results of the frame time analysis for representative exposures. The differences Δ in units of the 25 MHz quartz clocks compared to the CCF values are negligible for exposure times (e.g., 1 clock of 40 ns for SW mode per frame). However, the corrected numbers help to identify time jumps in the data over longer time spans – as deviations from integer number of frame times in time differences of two consecutive events can be detected more reliably.

While the values of M_1 are constant with time, the M_2 values contain an explicit relation to the EPIC-pn oscillator and implicitly to the onboard time (OBT) oscillator as trig-

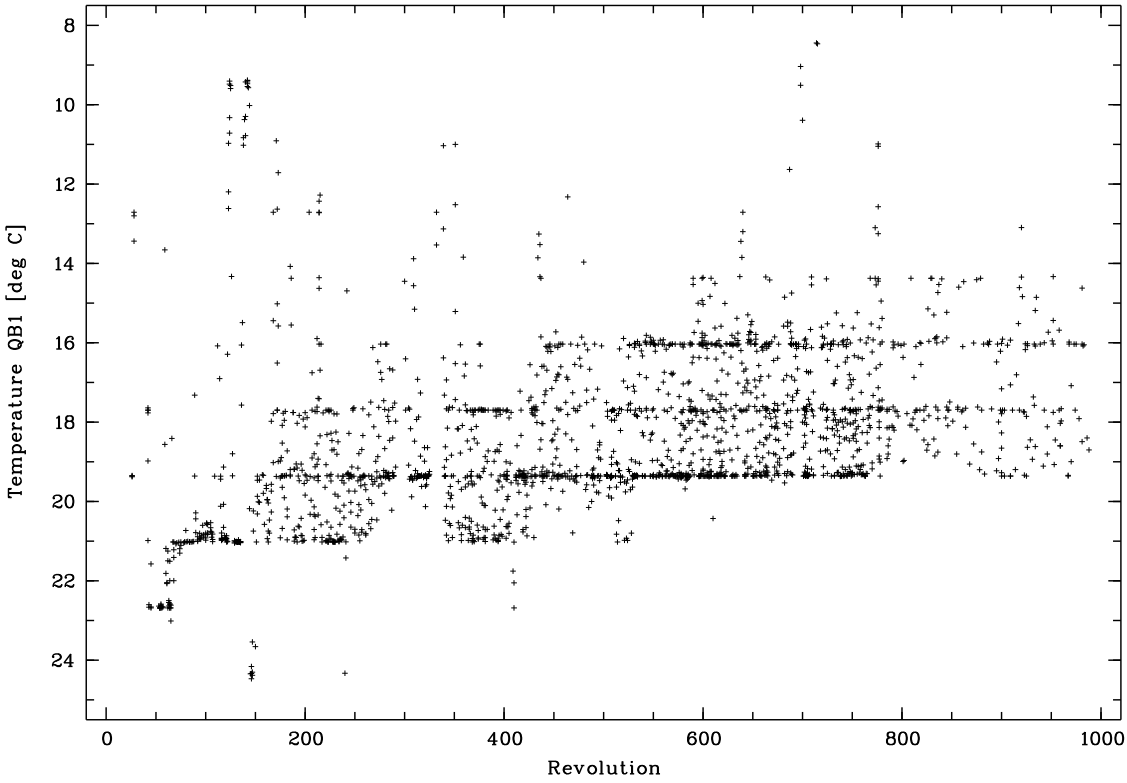

Fig. 3. Evolution of EPIC-pn quadrant box temperature for quadrant Q1 (which includes the target CCD) for FF mode, averaged over an exposure. The temperature sensor has only a coarse sampling (1 step = 0.88 °C), for shorter exposures only one value during an exposure is realized. The ordinate has been intentionally inverted, higher temperatures are toward the bottom. When comparing with Fig. 2 a similarity in terms of general trend is suggestive: a decreasing quadrant box temperature increases the frequency of the oscillator (which is not temperature stabilised).

ger of the full-second increment. Figure 2 shows the evolution of the effective EPIC-pn oscillator frequency with time expressed in XMM-*Newton* revolutions since launch, relative to the nominal 25 MHz frequency; the effect is not cumulative as after 1 second a reset is triggered externally. This plot does not use any time correlation such as corrections for OBT oscillator drifts (ageing, temperature). Kirsch et al. (2004) show that the OBT oscillator frequency decreases with time by only about 1 Hz per 30 revolutions; extrapolated to launch the deviation from nominal frequency ($2^{23} = 8388608$ Hz) was already -44.5 Hz, i.e. $-5.3\,10^{-6}$; after 1000 revolutions a total additional change of -25 Hz (i.e. $-3\,10^{-6}$) is expected.

It is unknown yet how much temperature changes in the EPIC-pn environment influence the EPIC-pn oscillator. The corresponding total change of the effective EPIC-pn frequency is about $+180$ Hz (i.e. $+7.2\,10^{-6}$). It is therefore likely that the dominating effect of the effective frequency shift is due to the EPIC-pn oscillator (e.g., ageing, temperature). In Fig. 2 there are external influences visible, like switch-off of RGS at revolutions $110 - 180$ or CDMU resets. The external OBT effects are corrected for using time correlation analysis. It is known that the EPIC-pn quadrant box temperatures generally decrease with time, which is believed to be due to cooler satellite environment caused by reduced reflected emission from Earth at perigee. Figure 3 shows the temperature of quadrant box Q1 averaged over an exposure from launch until present, with inverted ordinate. The temperature is decreasing (with a slope of about 3.2 mK per revolution for revolutions > 150); there is an apparent similarity to the trend in Fig. 2.

There is at the moment no tool in XMMSAS to correct for EPIC-pn internal oscillator drifts; note that this is not really needed for normal timing analysis as this small effect is limited to times within a second.

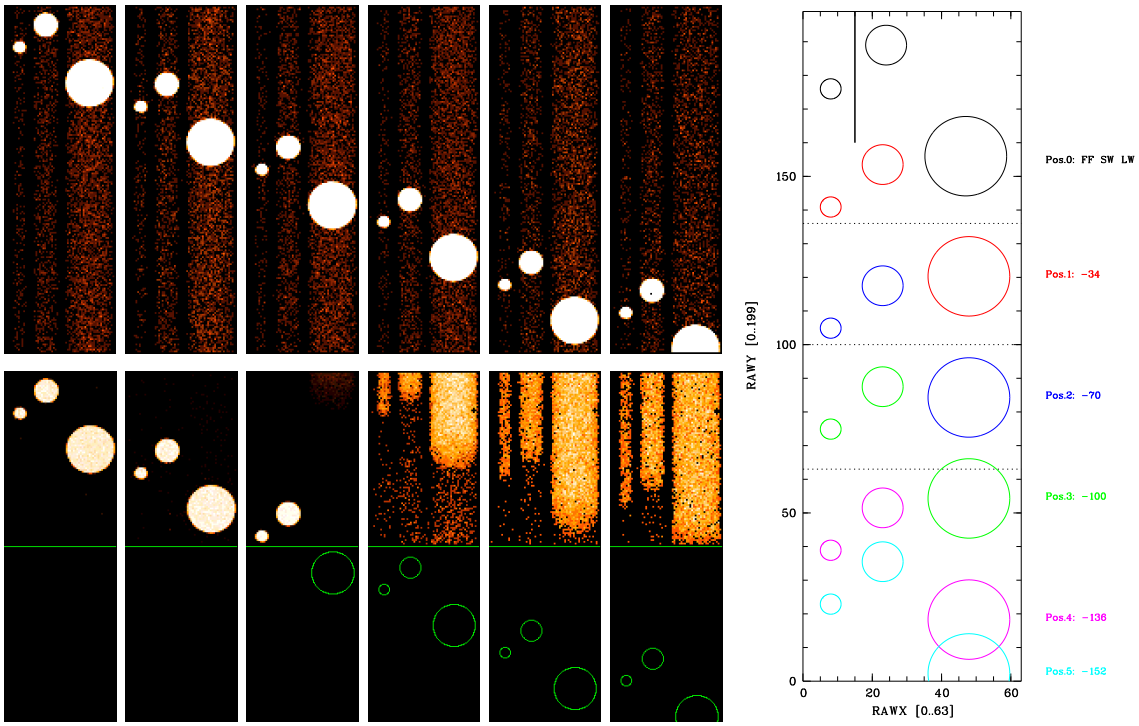

Fig. 4. *Right:* design of pinhole measurements at the Panter X-ray test facility: 3 pinholes with different sizes (4, 2, 1 mm $\sim$ 1.83, 0.92, 0.46 arcmin diameter) disjunct in `RAWX` and `RAWY` coordinates are moved relative to the FS camera into positions characteristic for various imaging modes. Each colour represents a certain position. The read-out is toward the bottom. *Top row:* intensity images for these 6 positions for CCD 4 in FF mode. *Bottom row:* as above but for LW mode; the green circles show the positions of the pinholes in front of the CCD.

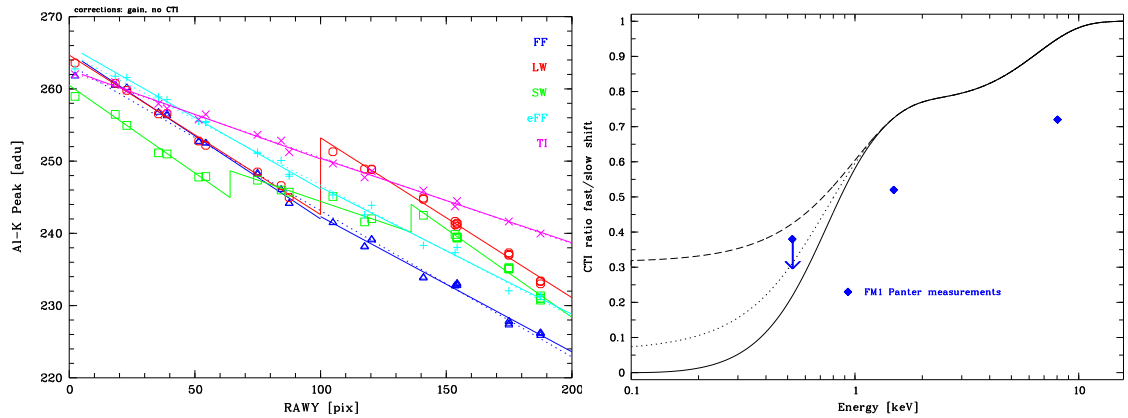

Fig. 5. *Left:* pinhole measurements for the FM1 camera at Al-K for various instrument modes. *Right*: comparison of the fast shift CTI contribution for FS (lines: CCF models) and FM1 (dots: Panter measurements).

4. EPIC-pn window mode CTI correction

The SW and LW modes are a sequence of an integration period, a fast shift of the integration window to the read-out node, then a slow read-out like in FF mode, and finally another (erase) fast shift of the window. Times are for LW mode for integration of 100-row window (45.14 ms), fast shift of window area toward CAMEX (0.072 ms, twice), and read-out as in full frame mode (2.45 ms). Charge transfer losses are consequently attributed to fast shift CTI and

to normal (slow) shift CTI. Using pinhole masks on ground dedicated areas of the CCD can be separately illuminated with monochromatic X-rays (for details see Freyberg et al. (2005)). The resulting peak positions (corrected for gain column variations only) can then be used to determine the CTI parameters.

A pinhole mask (2 mm Al) was put into the X-ray beam at the Panter facility in front of the EPIC-pn FM1 camera. Three holes with 1 mm, 2 mm, 4 mm diameters (for a focal length of 7.5 m this relates to 27.5″, 55″, 110″) were drilled disjointly in `RAWX` and `RAWY` projections so that they can be considered as independent. The EPIC-pn camera was then moved up and down behind the fixed mask to avoid any possible beam effects (like energy dispersion of monochromator). In Fig. 4 (left) we show images of FF and LW modes. The green circles in LW mode mark the positions of the pinholes above CCD 4, similarly to the FF mode. On the right-hand side the various pinhole positions are indicated with different colours.

With various line positions (corrected for column gain variations, in adu) of monochromatic input as function of position for various instrument modes we can derive the CTI losses for fast shifts and slow read-out. For LW mode, e.g., we have for `CTE = 1 - CTI`:

$Y > 100$:

$$\mathtt{PHA}(Y) = \mathtt{PHA}_0 \times \mathtt{CTE}_{\mathrm{fast}}^{100} \times \mathtt{CTE}_{\mathrm{slow}}^{Y-100}$$

$Y < 100$:

$$\mathtt{PHA}(Y) = \mathtt{PHA}_0 \times \mathtt{CTE}_{\mathrm{slow}}^{Y}$$

This leads to the relation

$$\mathtt{PHA}(Y)/\mathtt{PHA}(Y-100) = \mathtt{CTE}_{\mathrm{fast}}^{100}$$

and therefore

$$\mathtt{CTE}_{\mathrm{fast}} = (\mathtt{PHA}(Y)/\mathtt{PHA}(Y-100))^{1/100}$$

In window modes the peak positions show characteristic steps which are related to the difference between fast and slow shift losses (see Fig. 5 (left)). The gain (as determined from the amplitude value at `RAWY = 0`) seems to be slightly mode dependent for the FM1 camera. Figure 5 (right)) compares CCF values for the fast shift CTI contribution for the FS camera with ground measurements for the FM1 camera.

The pinhole procedure has been successfully applied to the FM1 camera model. As the operating conditions as well as detailed CCD properties are different, an in-orbit verification measurement is necessary. An extended multi-line target with intensities below pile-up is well-suited, such an example is N132D. Such a verification measurement was performed but background conditions were very high and thus spectral parameters (i.e. line shifts) could not be derived (the verification observation was repeated after this meeting, NRCO-47).

5. Conclusions

The EPIC-pn low-energy background is dominated by electronic read-out noise. Effects of possible sub-threshold pile-up will further be investigated (NRCO-49). Nominal EPIC-pn frame times in the CCFs (`EPN_TIMECORR`) will be revised; this will hopefully lead to significant improvements in the detection of time anomalies by the XMMSAS OAL library. The EPIC-pn fast shift CTI correction will be further analysed using an in-orbit calibration measurement (NRCO-47).

Acknowledgements. The XMM-*Newton* project is supported by the Bundesministerium für Bildung und Forschung / Deutsches Zentrum für Luft- und Raumfahrt (BMBF/DLR), the Max-Planck-Gesellschaft (MPG) and the Heidenhain-Stiftung.

References

Freyberg, M.J., Burkert, W., Hartner, G., Kirsch, M. 2005, Calibration Report, `ftp://epic3.xra.le.ac.uk/pub/cal-pv/meetings/mallorca-2005-02/mf_fastshiftcti.pdf`

Kirsch, M.G.F., Becker, W., Benlloch-Garcia, S., Jansen, F.A., Kendziorra, E., Kuster, M., Lammers, U., Pollock, A.M.T., Possanzini, F., Serpell, E., Talavera, A. 2004, Proc. SPIE 5165, 85, `http://xmm.vilspa.esa.es/docs/documents/CAL-TN-0045-1-0.pdf`

Note added: In Tab.1 a typesetting error of the printed version has been corrected, with the proper recommended frame time value for the SW mode of 5.67180 ms, all other entries had been correct (especially the number of clocks, i.e. 141795 clocks of 40 ns each).